Supporting information

Improvement of the versatility of an arabinofuranosidase against galactofuranose for the synthesis of galactofuranoconjugates

Quentin Pavic[a], Aline Pillot[a], Olivier Tasseau[a], Laurent Legentil[a], and Sylvain Tranchimand[a]*

[a] Univ Rennes, Ecole Nationale Supérieure de Chimie de Rennes, CNRS, ISCR – UMR 6226, F-35000 Rennes, France
Tel: (+33)-223-238096, e-mail: sylvain.tranchimand@ensc-rennes.fr

List of supplementary information

Table S1: Primers used for saturation site-directed mutagenesis at positions 29, 319 and 357, and for point mutation at position 173.

Figure S1: Hydrogen bond networks of the complexes *p*NP-α-L-arabinofuranoside/*Ct*Ara*f*51 (A) and *p*NP-β-D-galactofuranoside/*Ct*Ara*f*51 (B) after docking.

Figure S2: Screening against *p*NP-β-D-galactofuranoside hydrolysis of the banks of mutants. A: L319X bank. B: L29X bank. C: I357X bank.

Figure S3: Docking of *p*NP-β-D-galactofuranoside in the active site of *Ct*Ara*f*51 WT (A); *Ct*Ara*f*51 L319V (B) and *Ct*Ara*f*51 L29V (C).

Figure S4: Hydrogen bond networks of the complexes *p*NP-β-D-galactofuranoside/*Ct*Ara*f*51 L319V (A) and *p*NP-β-D-galactofuranoside/*Ct*Ara*f*51 L29V (B) after a 10 ns MD.

Figure S5: NMR traces over time of the transglycosylation reaction using the L319V mutant (A), the L29V mutant (B) or the WT enzyme (C) as the biocatalyst.

Figure S6: NMR traces over time of the acylation reaction using the E173 L319V double mutant (A), the E173 L29V double mutant (B) or the E173A mutant (C) as the biocatalyst.

Figure S7: NMR traces over time of the thioligation reaction using the E173A L319V double mutant (A), the E173 L29V double mutant (B) or the E173A mutant (C) as the biocatalyst.

^{1}H and ^{13}C NMR spectrum of isolated ethyl galactofuranoside **4**, *p*-methoxybenzoyl galactofuranose **6** and thiophenyl galactofuranoside **7**.

Mutation	Primer
Leu29X	5'- GGCTCTTTTGTAGAACAT**NNN**GGAAGGGCCGTATATGACGG -3'
Leu319X	5'- GGAGAATAGCGCCTCCTTTA**NNN**GAGGATATATATACGTTTG -3'
Ile357X	5'- CTGGCACAGTTGATTAATGTA**NNN**GCGCCTATTGTGACTGAAAG -3'
Glu173Ala	5'- GGTGTCTTGGCAAT**GCC**ATGGACGGTCCG-3'

Table S1: Primers used for saturation site-directed mutagenesis at positions 29, 319 and 357, and for point mutation at position 173. Mutated codon is indicated in bold. Indicated primers and their reverse-complements were used for the mutagenesis reactions.

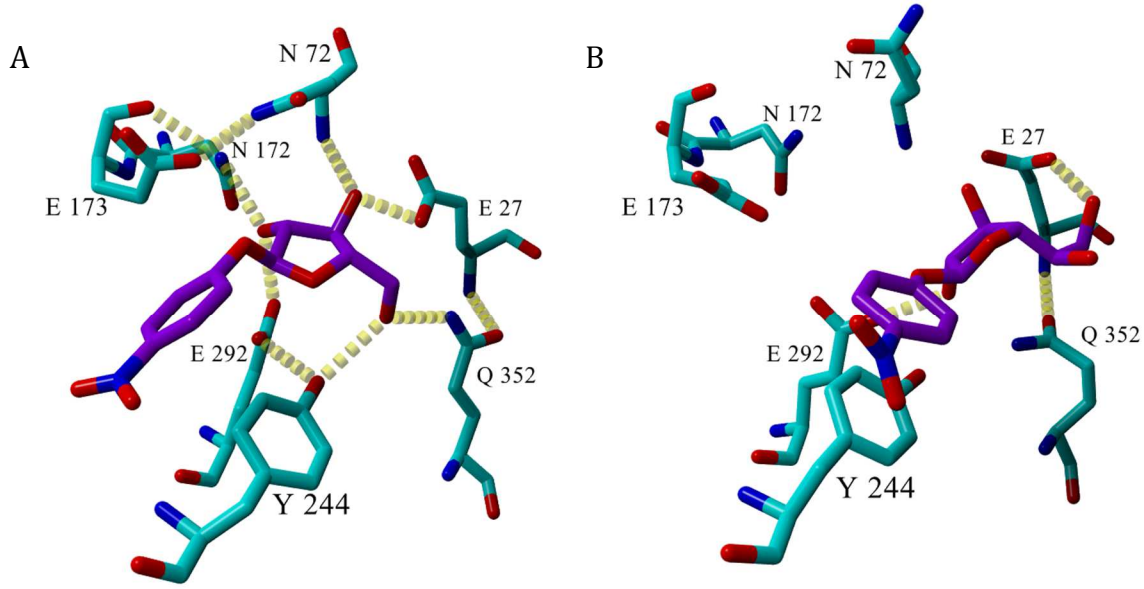

Figure S1. Hydrogen bond networks of the complexes *p*NP-α-L-arabinofuranoside/*Ct*Ara*f*51 (A) and *p*NP-β-D-galactofuranoside/*Ct*Ara*f*51 (B) after docking.

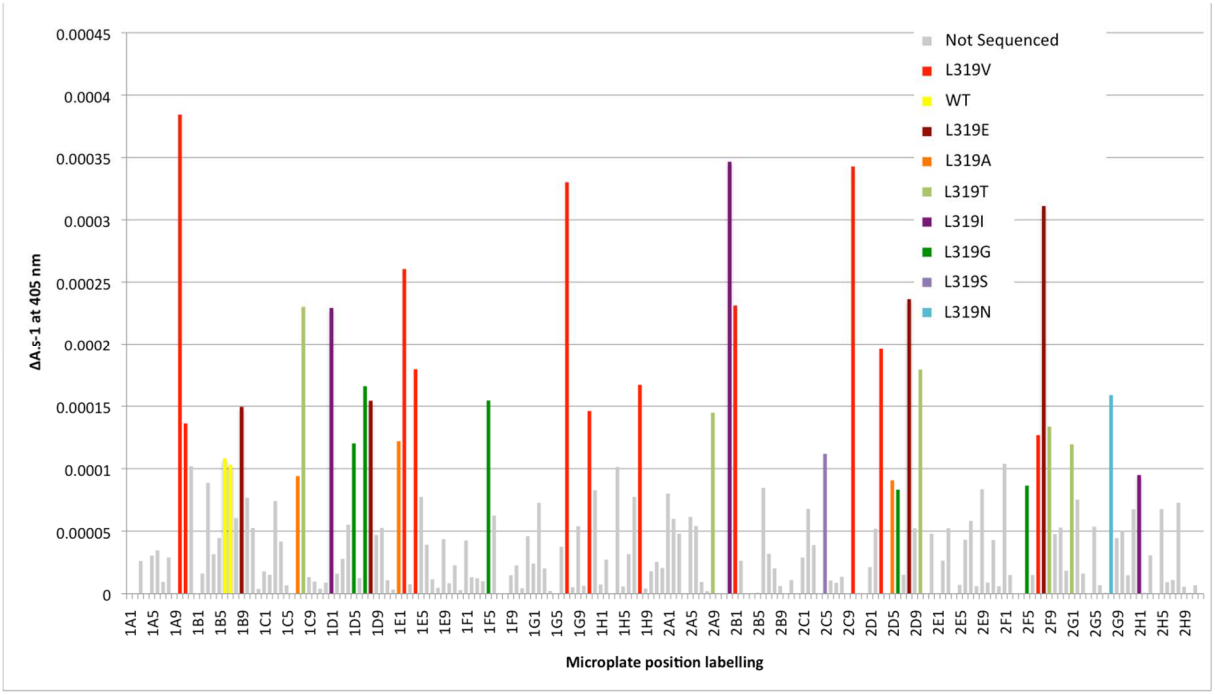

Figure S2A. Screening against *p*NP-β-D-galactofuranoside hydrolysis of the L319X bank. Activities are reported as the slopes of the kinetic measurement at 405 nm over 30 min at 25°C and pH 7.

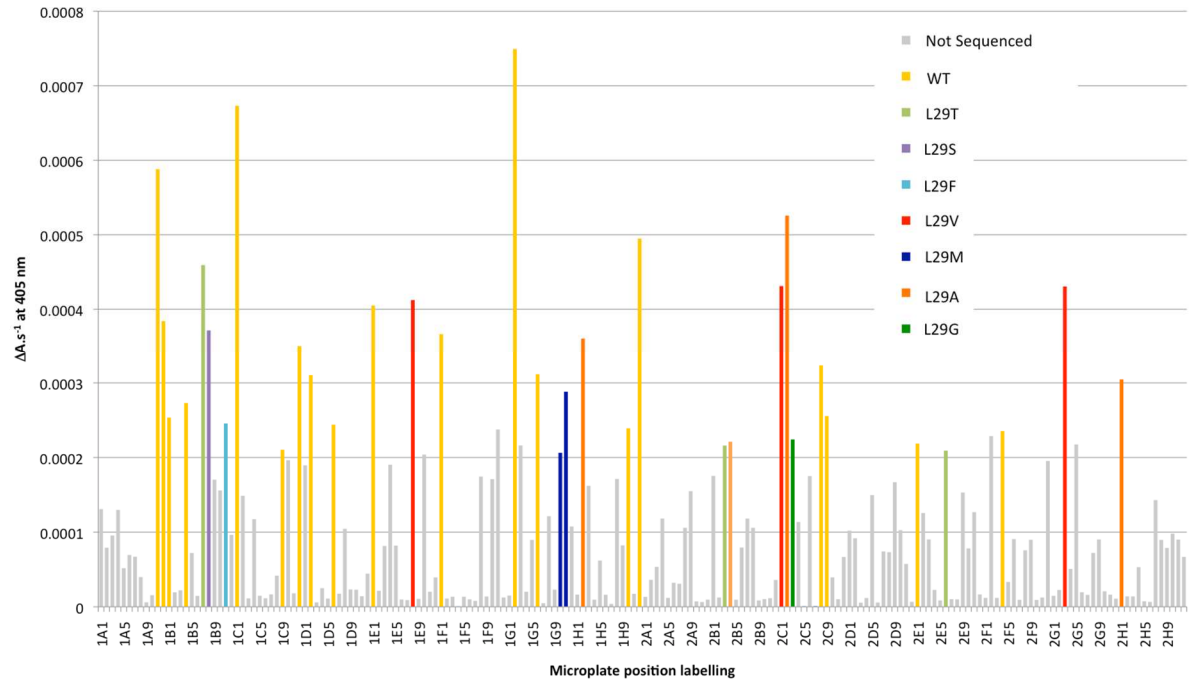

Figure S2B. Screening against *p*NP-β-D-galactofuranoside hydrolysis of the L29X bank. Activities are reported as the slopes of the kinetic measurement at 405 nm over 30 min at 25°C and pH 7.

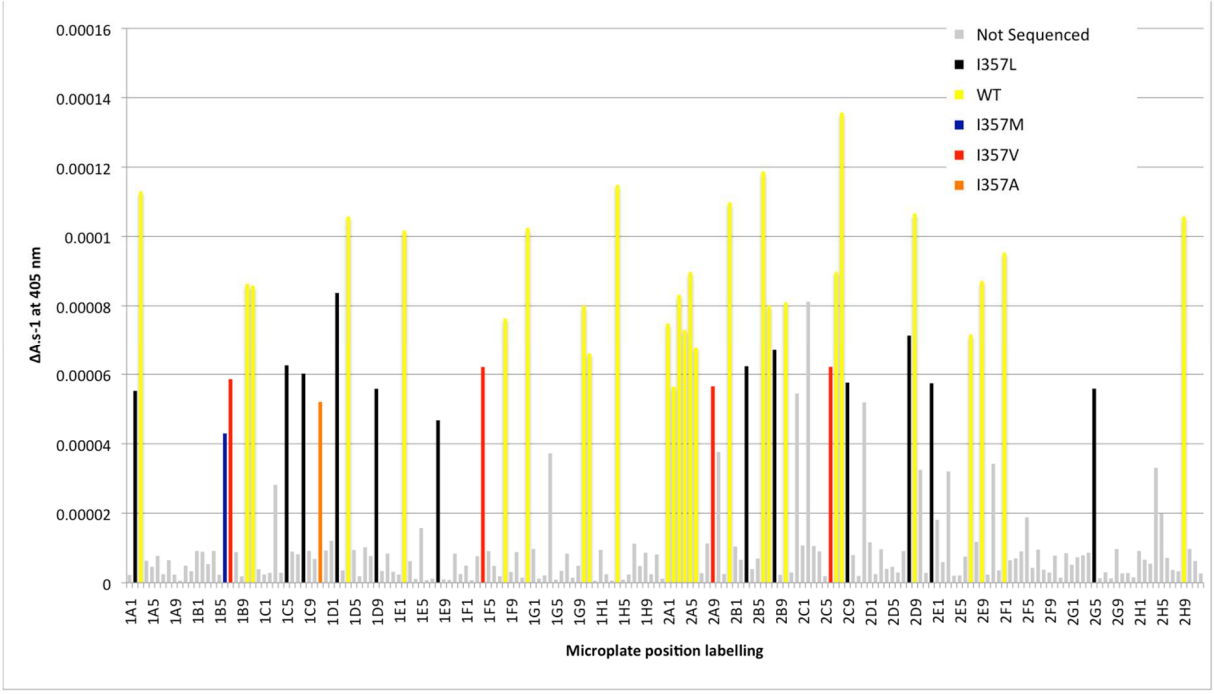

Figure S2C. Screening against *p*NP-β-D-galactofuranoside hydrolysis of the I357X bank. Activities are reported as the slopes of the kinetic measurement at 405 nm over 30 min at 25°C and pH 7.

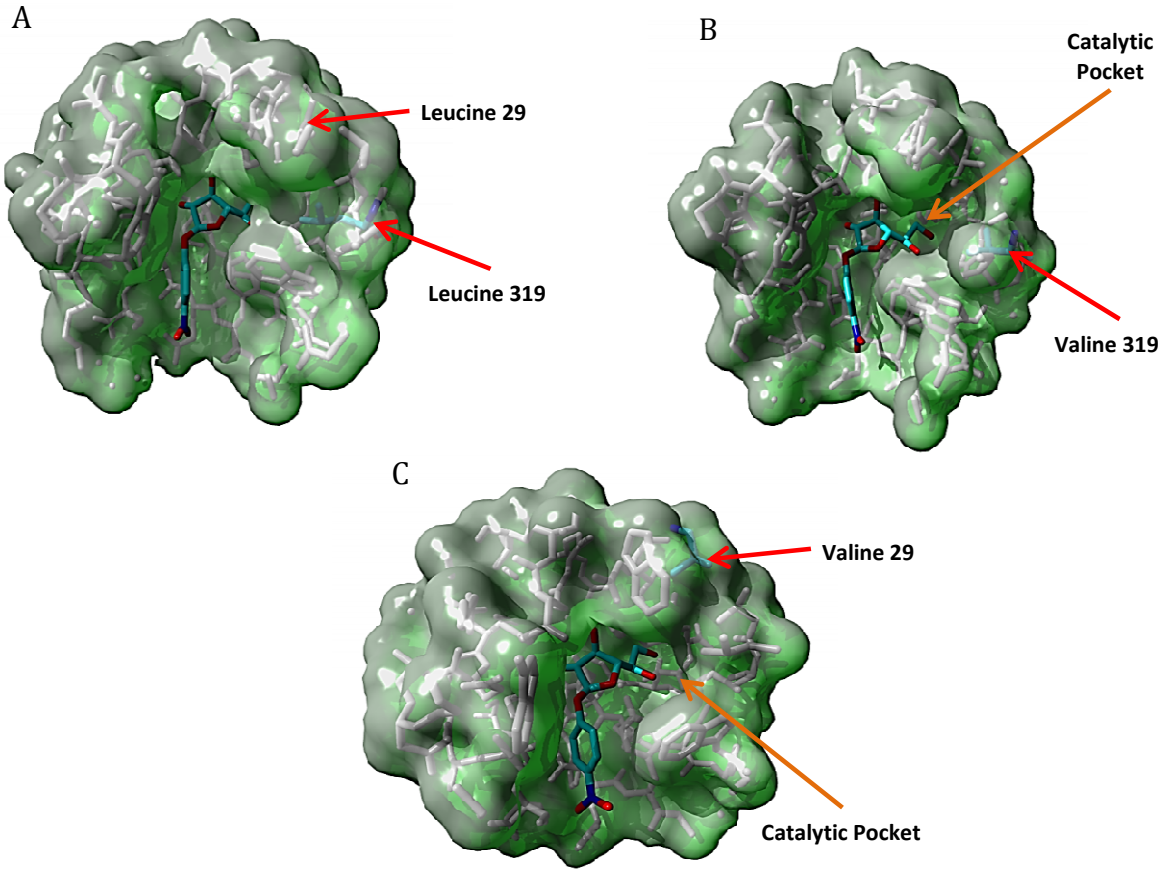

Figure S3. Docking of *p*NP-β-D-galactofuranoside in the active site of *Ct*Araf51 WT (A); *Ct*Araf51 L319V (B) and *Ct*Araf51 L29V (C).

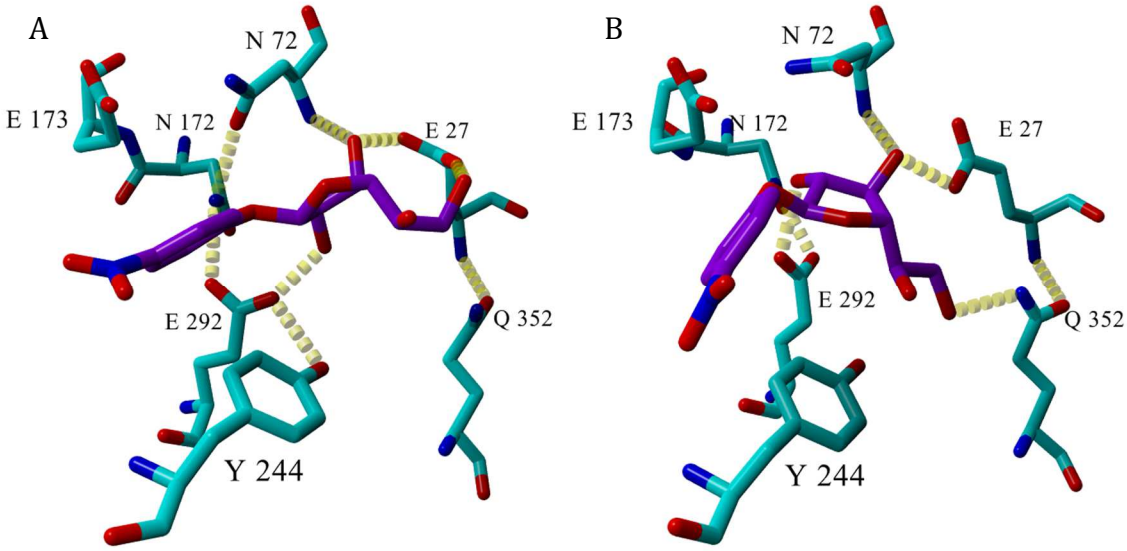

Figure S4. Hydrogen bond networks of the complexes *p*NP-β-D-galactofuranoside/*Ct*Araf51 L319V (A) and *p*NP-β-D-galactofuranoside/*Ct*Araf51 L29V (B) after a 10 ns MD.

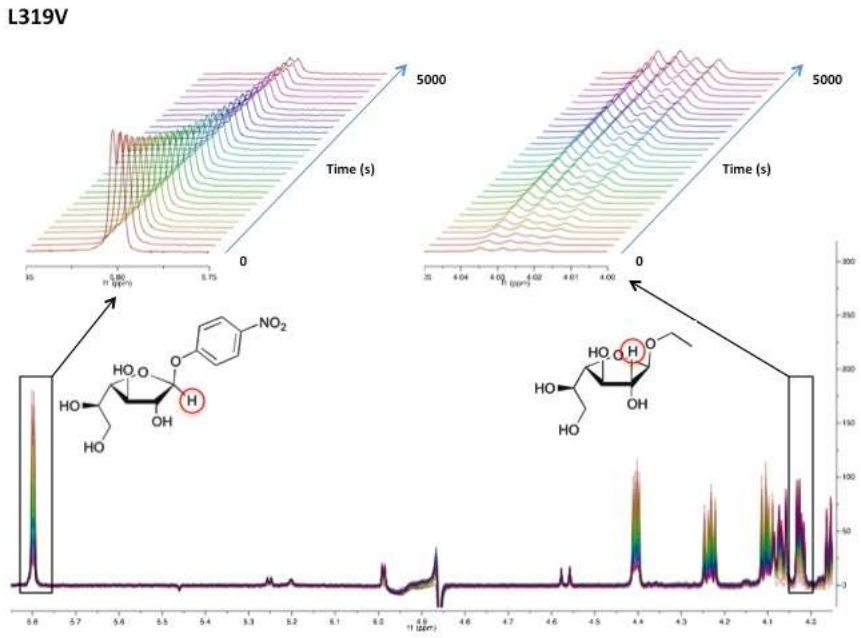

Figure S5A. NMR traces over time of the transglycosylation reaction using the L319V mutant as the biocatalyst.

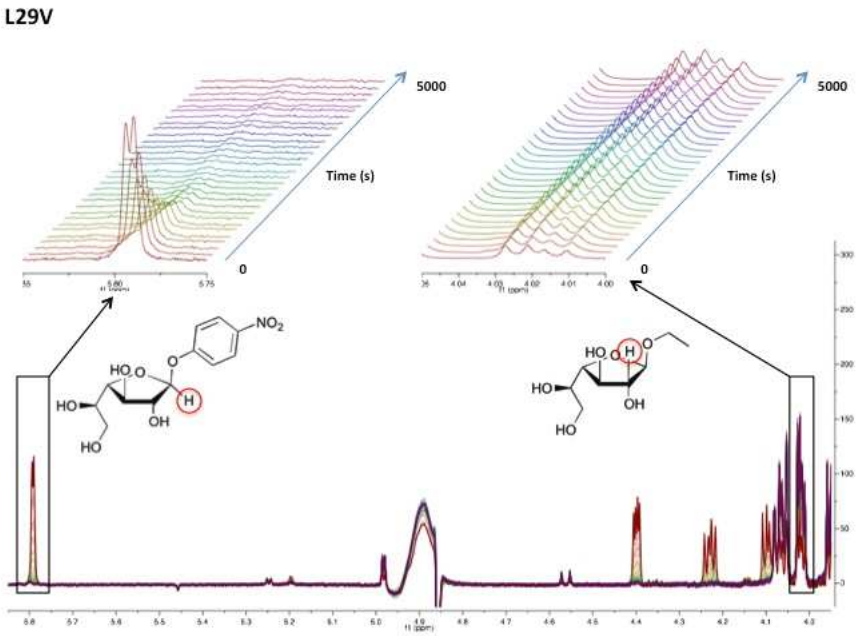

Figure S5B. NMR traces over time of the transglycosylation reaction using the L29V mutant as the biocatalyst.

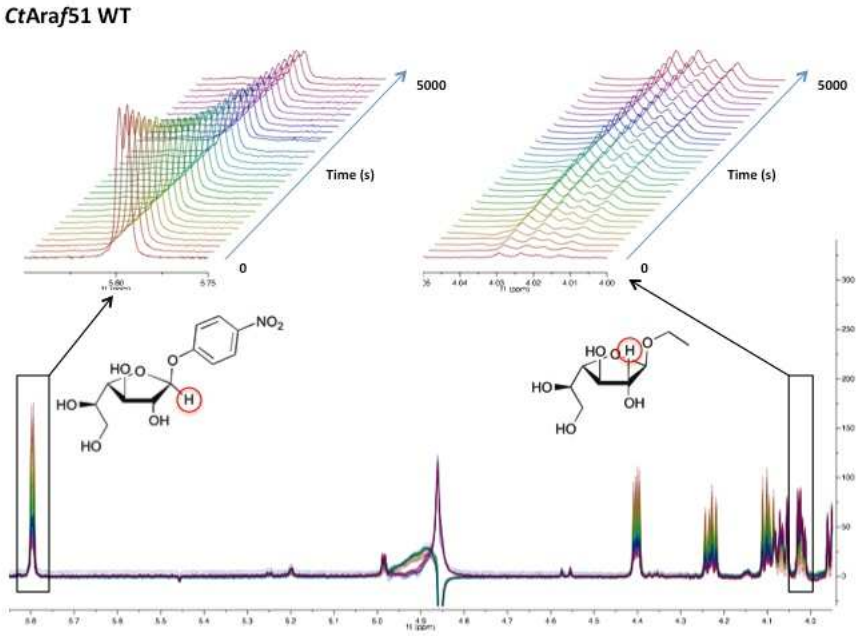

Figure S5C. NMR traces over time of the transglycosylation reaction using the WT *Ct*Ara*f*51 as the biocatalyst.

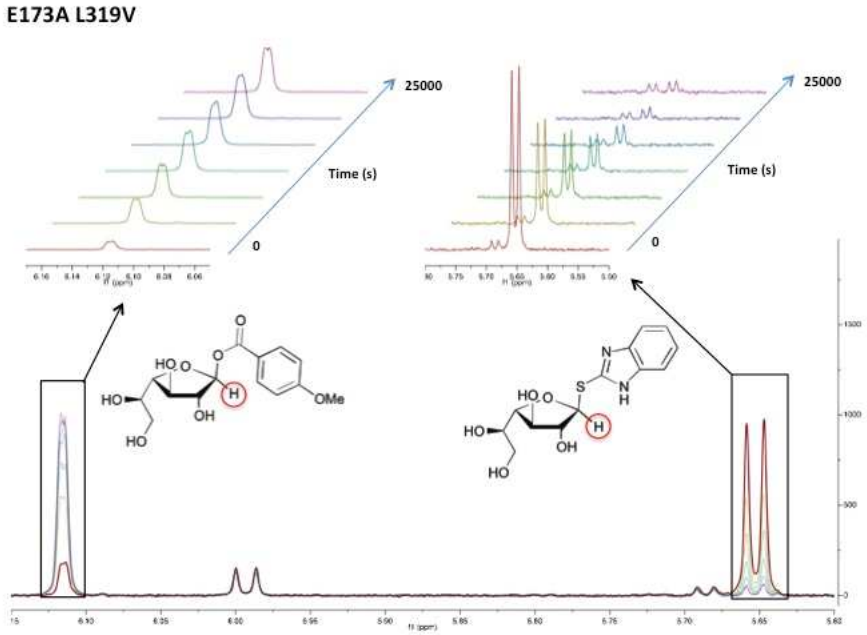

Figure S6A. NMR traces over time of the acylation reaction using the E173 L319V double mutant as the biocatalyst.

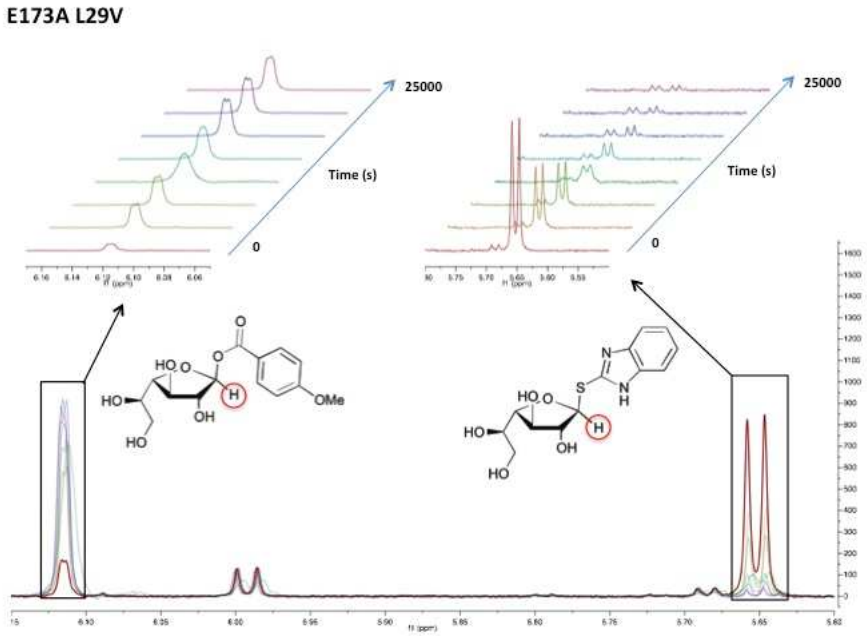

Figure S6B. NMR traces over time of the acylation reaction using the E173 L29V double mutant as the biocatalyst.

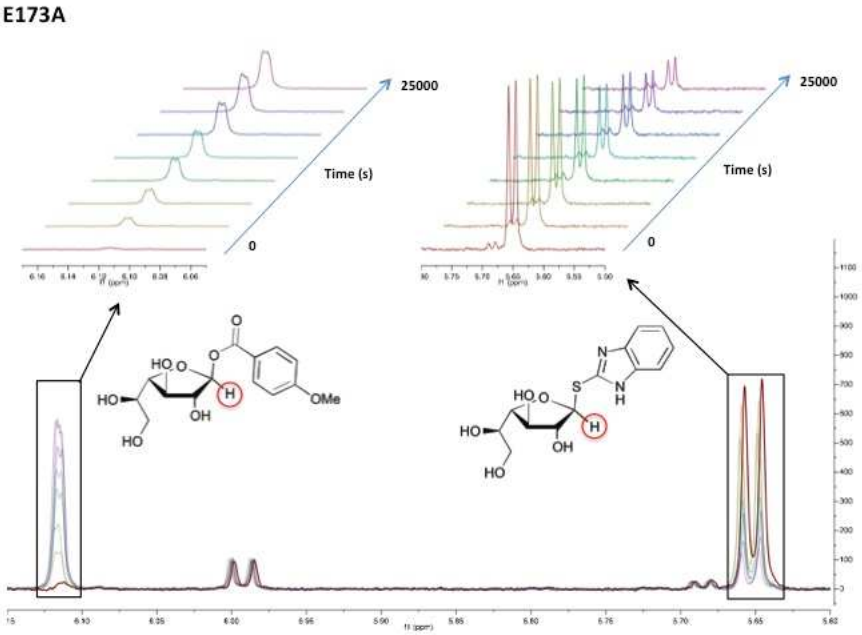

Figure S6C. NMR traces over time of the acylation reaction using the E173 mutant as the biocatalyst.

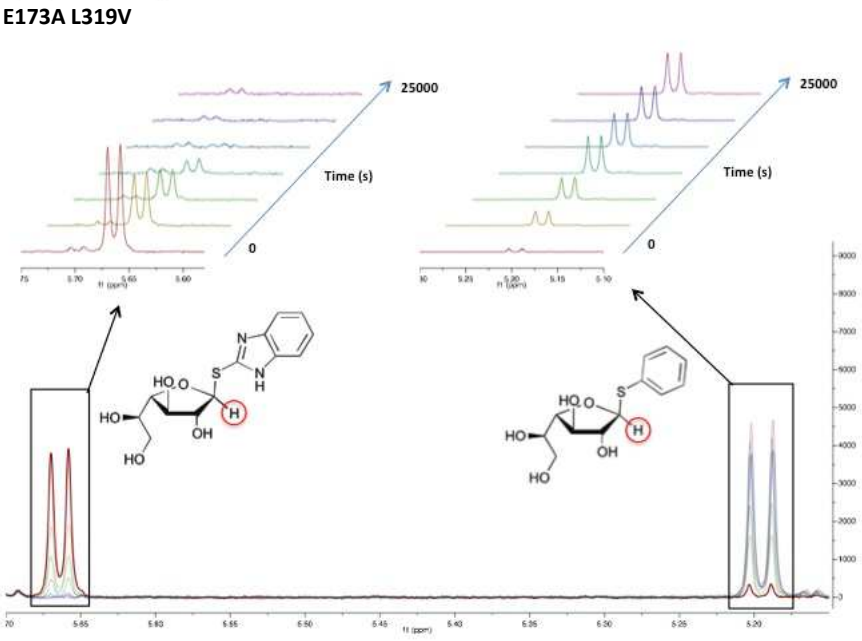

Figure S7A. NMR traces over time of the thioligation reaction using the E173A L319V double mutant as the biocatalyst.

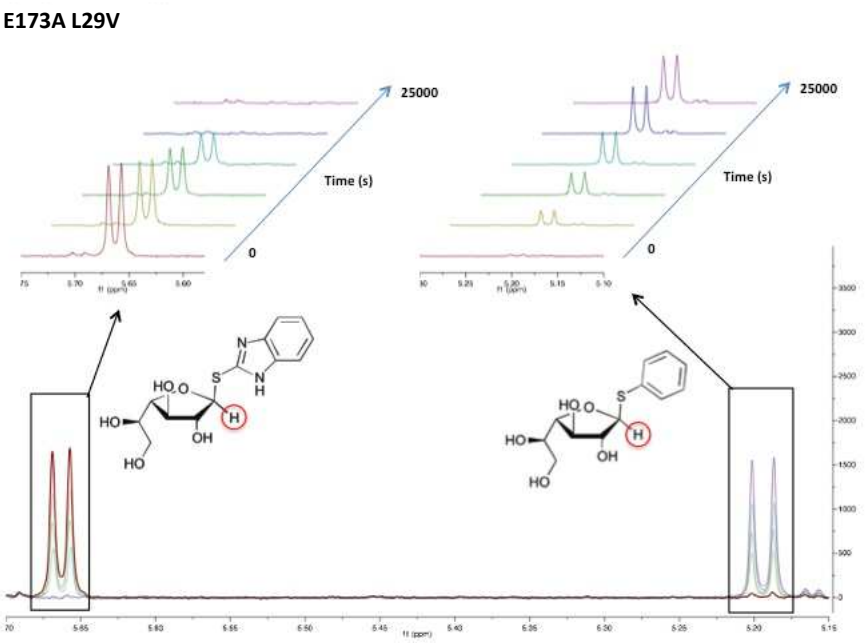

Figure S7B. NMR traces over time of the thioligation reaction using the E173A L29V double mutant as the biocatalyst.

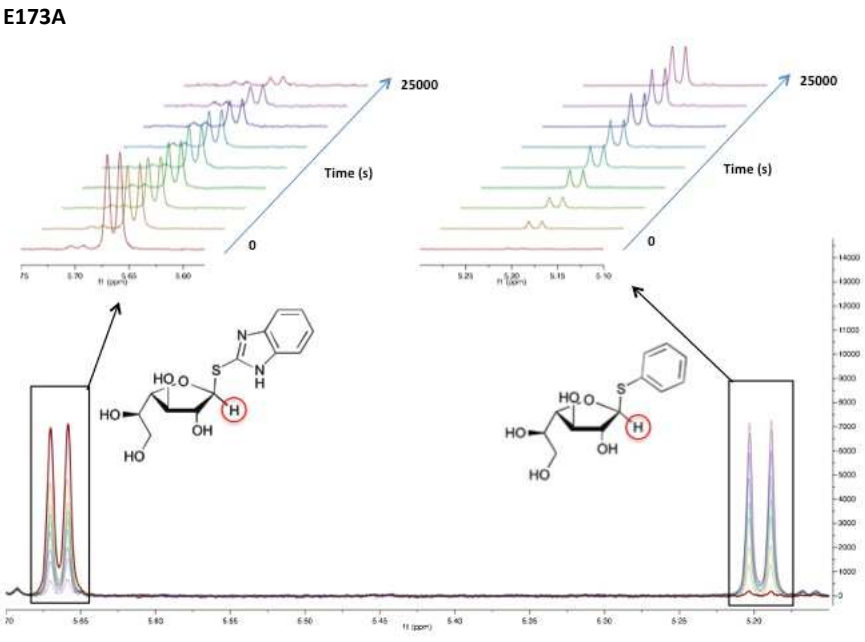

Figure S7C. NMR traces over time of the thioligation reaction using the E173A mutant as the biocatalyst.

^{1}H and ^{13}C NMR spectrum of isolated ethyl galactofuranoside **4**, *p*-methoxybenzoyl galactofuranose **6** and thiophenyl galactofuranoside **7**.

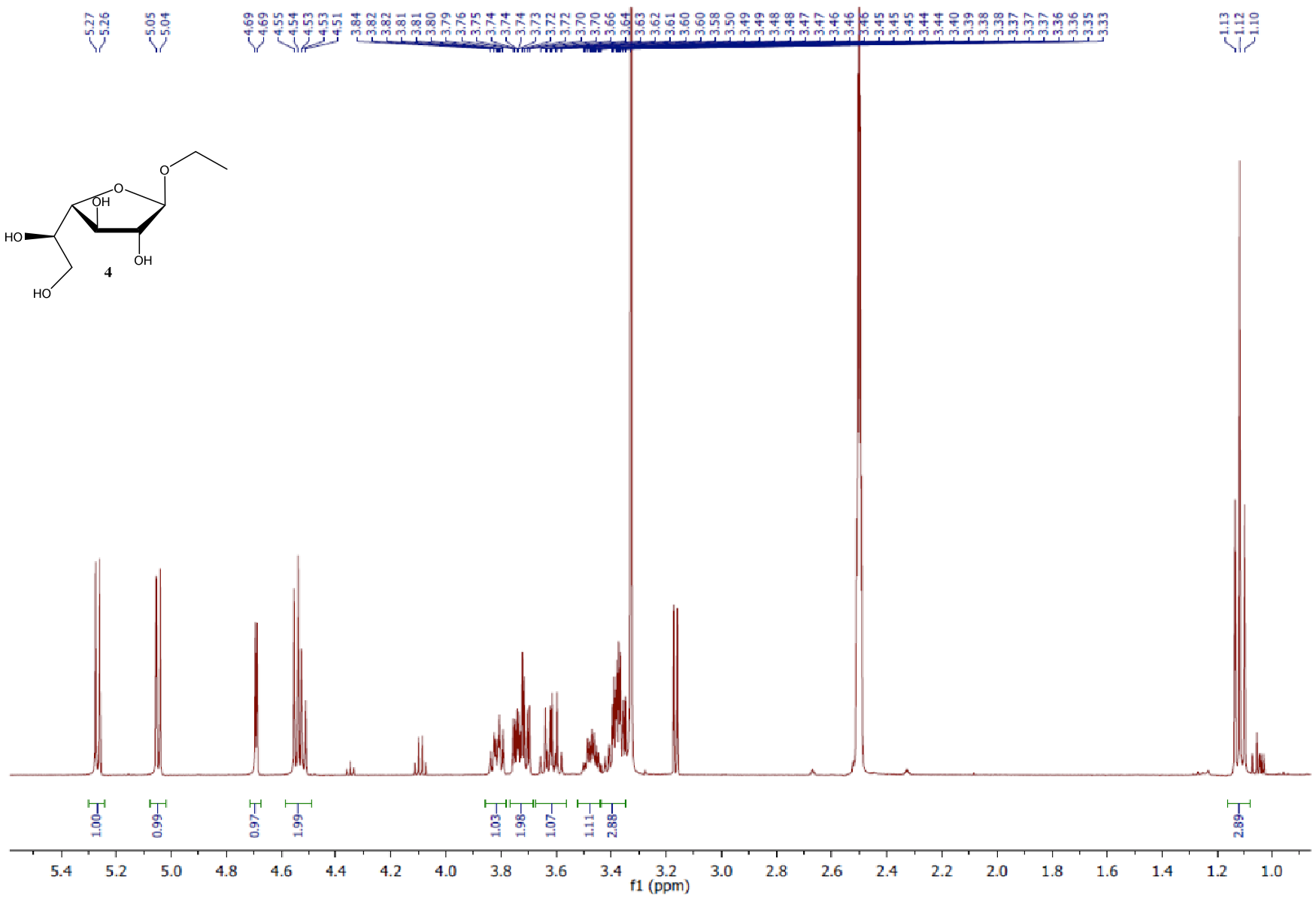
5.27
5.26
5.05
5.04
4.69
4.69
4.55
4.54
4.54
4.53
4.53
4.51
3.84
3.82
3.82
3.81
3.81
3.80
3.79
3.76
3.75
3.74
3.74
3.74
3.73
3.72
3.72
3.70
3.70
3.66
3.64
3.63
3.62
3.61
3.60
3.60
3.58
3.50
3.49
3.49
3.48
3.48
3.47
3.47
3.46
3.46
3.46
3.45
3.45
3.45
3.44
3.44
3.40
3.39
3.38
3.37
3.37
3.37
3.36
3.35
3.33
1.13
1.12
1.10
O
OH
O
HO
OH
HO
4
1.00
0.99
0.97
1.99
1.03
1.98
1.07
1.11
2.88
2.89
5.4
5.2
5.0
4.8
4.6
4.4
4.2
4.0
3.8
3.6
3.4
3.2
3.0
2.8
2.6
2.4
2.2
2.0
1.8
1.6
1.4
1.2
1.0
f1 (ppm)

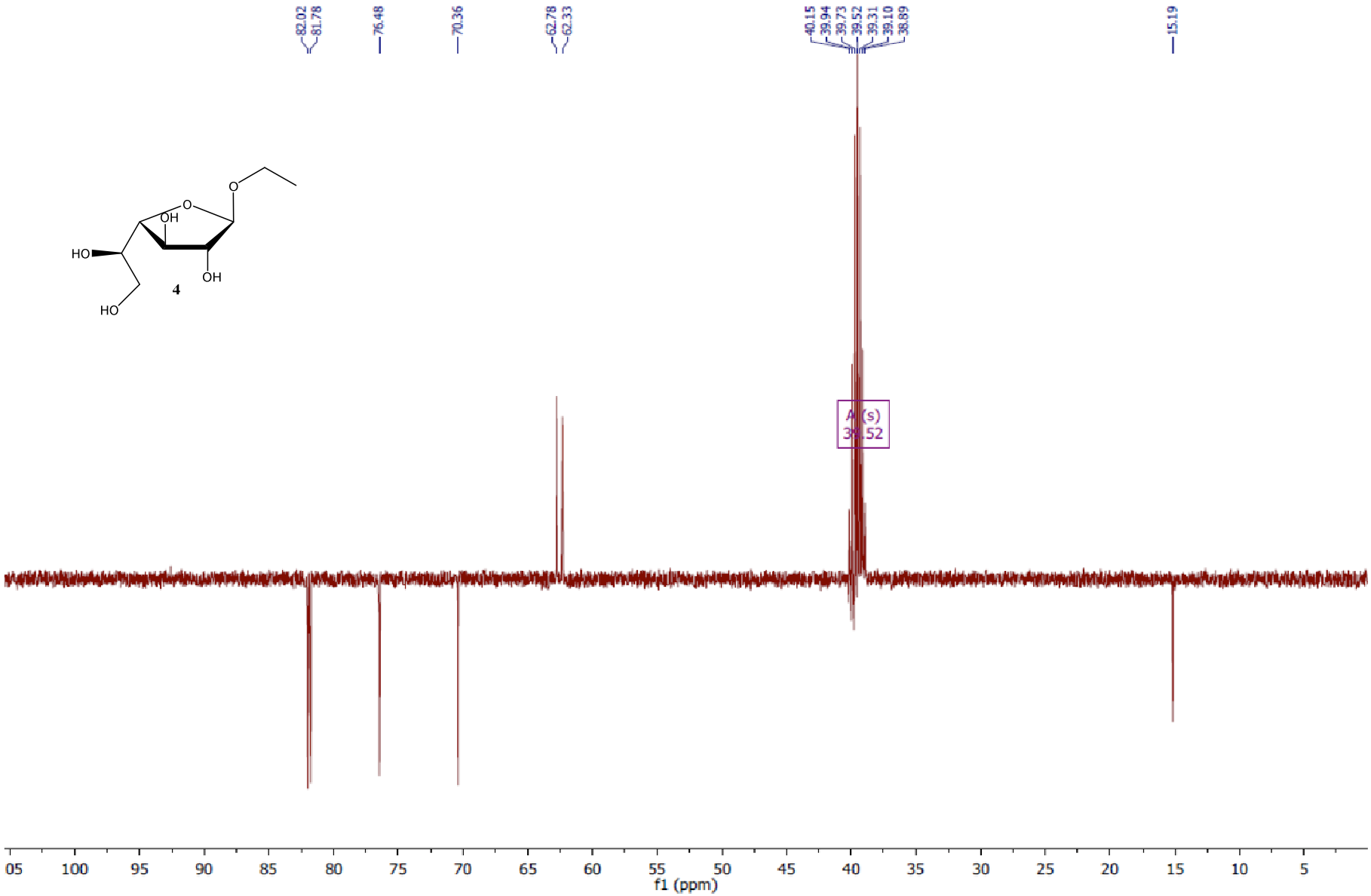
82.02
81.78
76.48
70.36
62.78
62.33
40.15
39.94
39.73
39.52
39.31
39.10
38.89
15.19
HO
OH
O
O
OH
HO
4
A (s)
05
100
95
90
85
80
75
70
65
60
55
50
45
40
35
30
25
20
15
10
5
f1 (ppm)

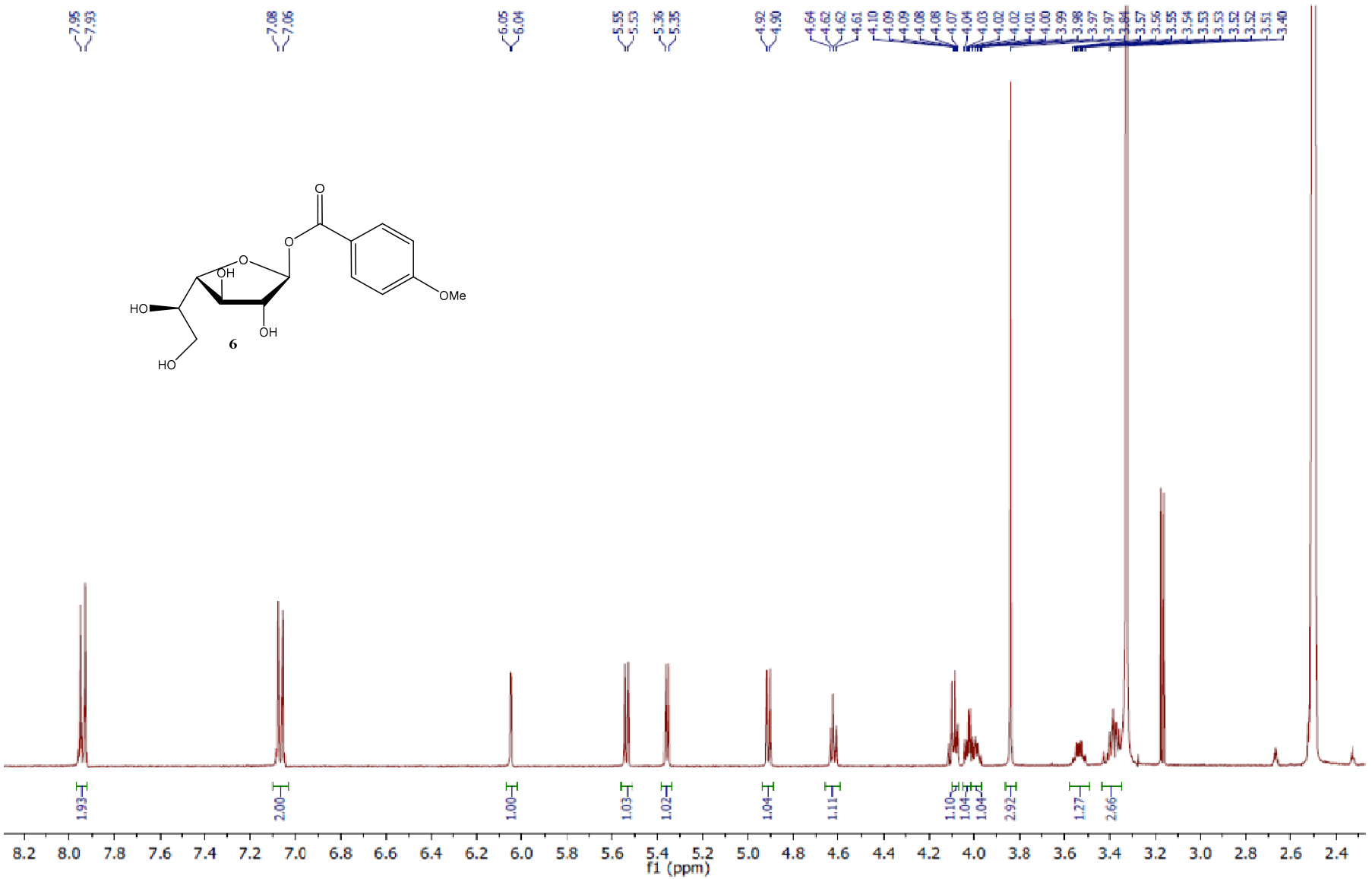
7.95
7.93
7.08
7.06
6.05
6.04
5.55
5.53
5.36
5.35
4.92
4.90
4.64
4.62
4.62
4.61
4.10
4.09
4.09
4.08
4.08
4.07
4.04
4.03
4.02
4.02
4.01
4.00
3.99
3.98
3.97
3.97
3.84
3.57
3.56
3.55
3.54
3.53
3.52
3.52
3.51
3.40
O
O
OH
O
HO
OH
HO
OMe
6
1.93
2.00
1.00
1.03
1.02
1.04
1.11
1.10
1.04
1.04
2.92
1.27
2.66
8.2
8.0
7.8
7.6
7.4
7.2
7.0
6.8
6.6
6.4
6.2
6.0
5.8
5.6
5.4
5.2
5.0
4.8
4.6
4.4
4.2
4.0
3.8
3.6
3.4
3.2
3.0
2.8
2.6
2.4
f1 (ppm)

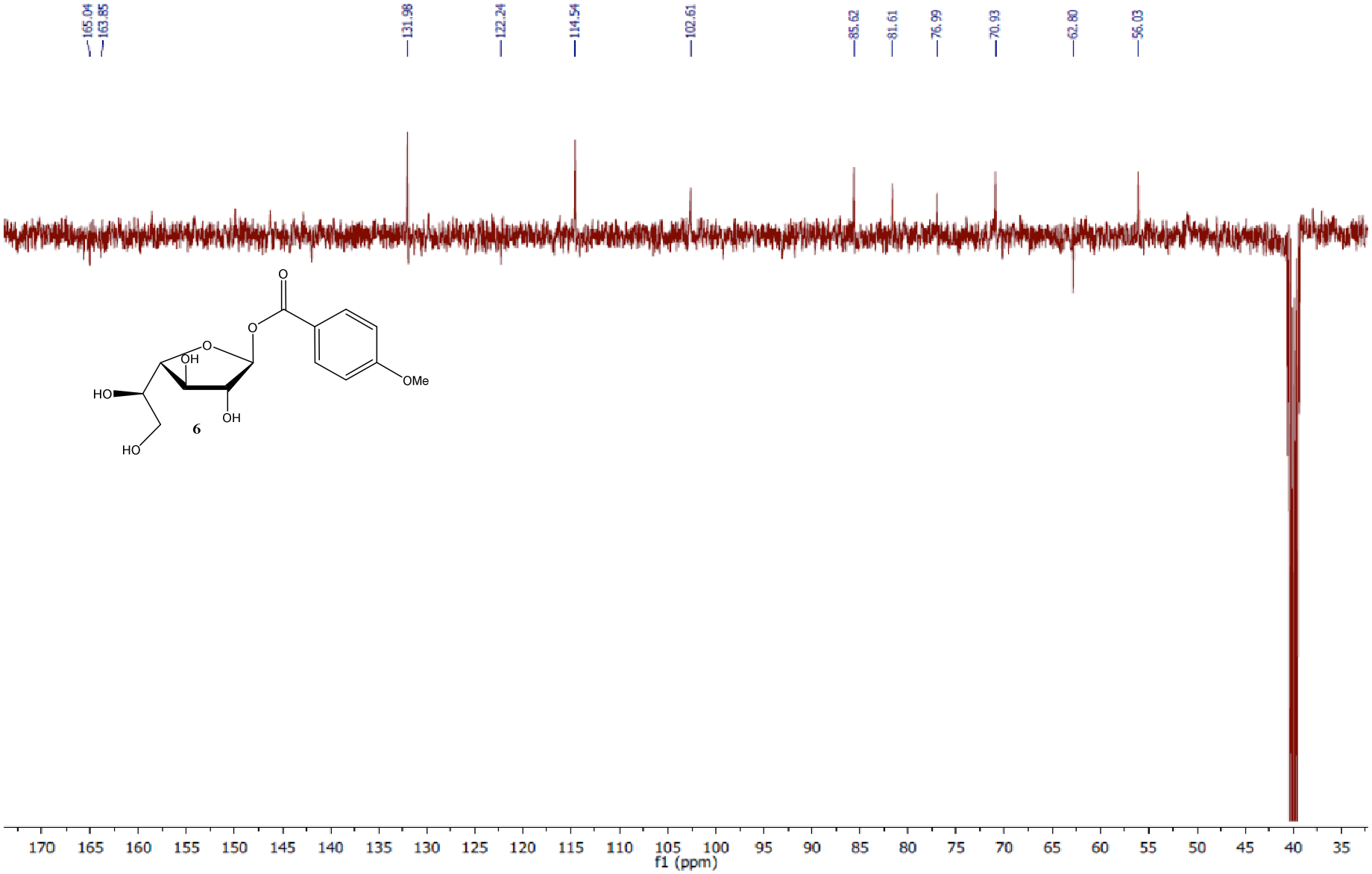
165.04
163.85
131.98
122.24
114.54
102.61
85.62
81.61
76.99
70.93
62.80
56.03
O
O
O
OH
HO
OH
HO
OMe
6
170 165 160 155 150 145 140 135 130 125 120 115 110 105 100 95 90 85 80 75 70 65 60 55 50 45 40 35
f1 (ppm)

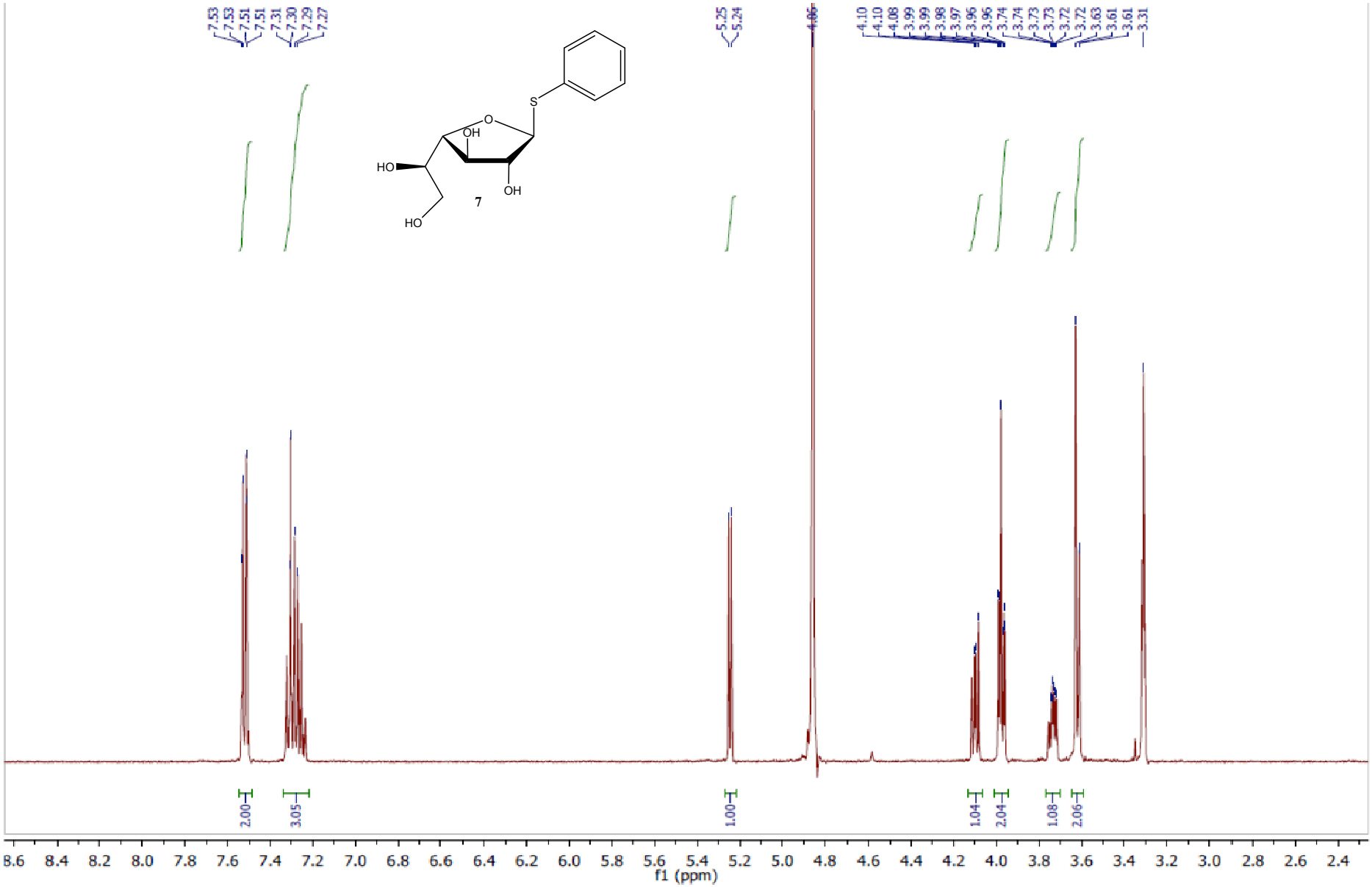
7.53
7.53
7.51
7.51
7.31
7.30
7.29
7.27
5.25
5.24
4.86
4.10
4.10
4.08
3.99
3.99
3.98
3.97
3.96
3.96
3.74
3.74
3.73
3.73
3.72
3.72
3.63
3.61
3.61
3.31
O
S
OH
HO
OH
HO
7
2.00
3.05
1.00
1.04
2.04
1.08
2.06
8.6 8.4 8.2 8.0 7.8 7.6 7.4 7.2 7.0 6.8 6.6 6.4 6.2 6.0 5.8 5.6 5.4 5.2 5.0 4.8 4.6 4.4 4.2 4.0 3.8 3.6 3.4 3.2 3.0 2.8 2.6 2.4
f1 (ppm)

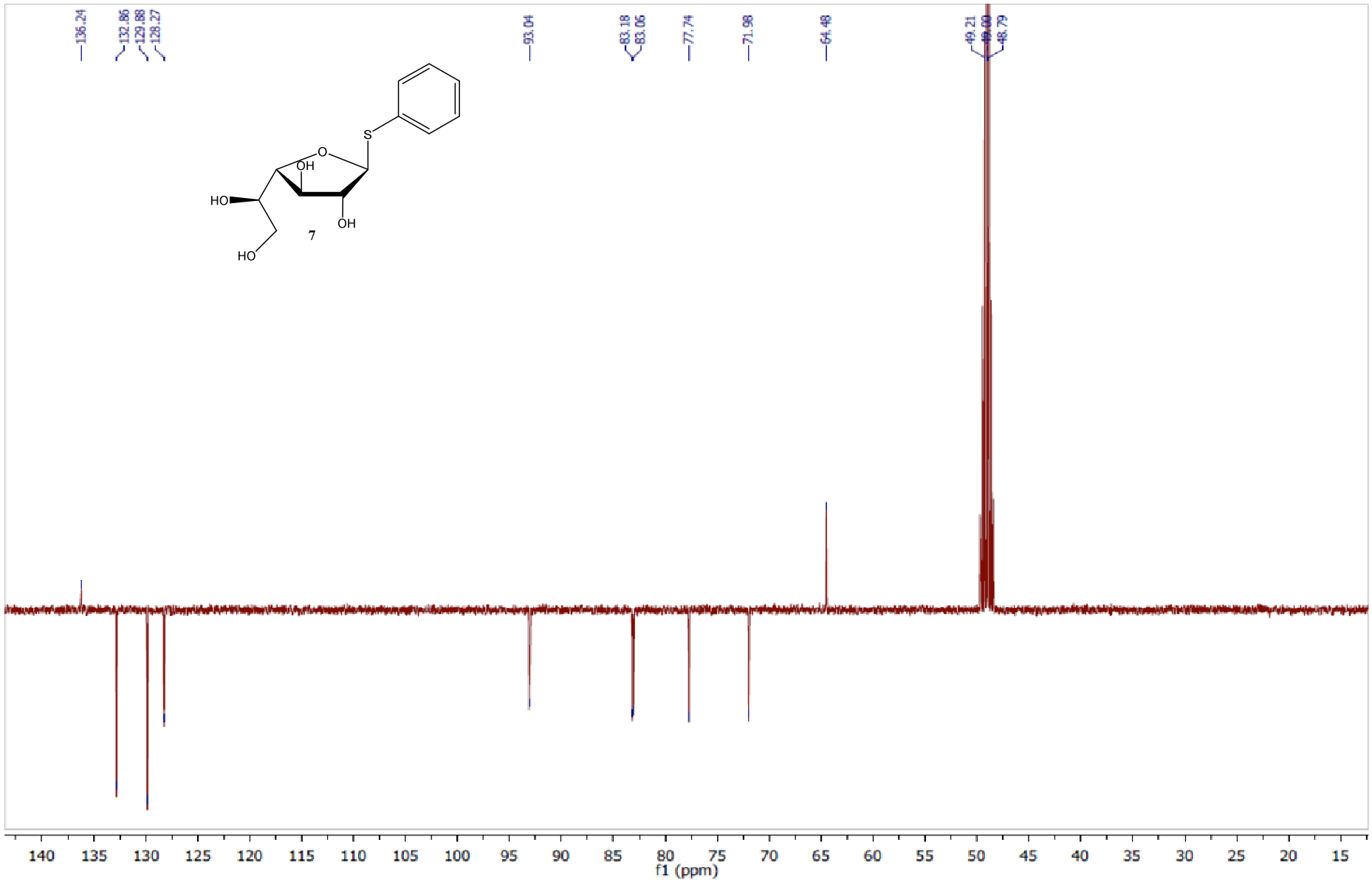
136.24
132.86
129.88
128.27
93.04
83.18
83.06
77.74
71.98
64.48
49.21
49.00
48.79
O
S
OH
HO
OH
HO
7
140
135
130
125
120
115
110
105
100
95
90
85
80
75
70
65
60
55
50
45
40
35
30
25
20
15
f1 (ppm)